Available Online at http://www.journalajst.com

ISSN: 0976-3376

ASIAN JOURNAL OF SCIENCE AND TECHNOLOGY

Asian Journal of Science and Technology
Vol. 17, Issue, 06, pp. 14360-14367, June, 2026

RESEARCHARTICLE

TECTONIC EVOLUTION OF THE IVORIAN BIRIMIAN BASEMENT: INSIGHTS FROM MESOSTRUCTURAL ANALYSIS OF THE KAN GRANITO-GNEISSIC COMPLEX AND THE COMOÉ METASEDIMENTS (CENTRAL-EASTERN CÔTE D'IVOIRE)

Koffi Kossonou Jean-Marie PRIA[1], Konan Roger ASSIE[1]*, Krohognon FOFANA[1]

[1]Jean Lorougnon Guédé University, Faculty of Environment, Department of Earth Sciences, Laboratory of Environmental Sciences and Technologies, BP 150, Daloa, Côte d'Ivoire

ARTICLE INFO

Article History:
Received 24th March, 2026
Received in revised form
16th April, 2026
Accepted 28th May, 2026
Published online 30th June, 2026

Keywords:
Polyphased tectogenesis; Sinistral and dextral shear zones; Comoé metasediments; Kan granito-gneissic complex; Brobo shear zone and Dimbokro fault; Ductile and brittle deformation.

***Corresponding author:**
Konan Roger ASSIE

ABSTRACT

The Birimian basement of Côte d'Ivoire is characterized by a complex tectono-metamorphic history, yet the structural evolution of the Kan granito-gneissic complex (KGC) and the Comoé metasediments (CMS) remains insufficiently documented. This study combines teleanalytic mapping with field-based structural measurements to reconstruct the tectonic evolution of these formations. Lineament analysis highlights four principal orientations (E-W, N-S, NE-SW, NW-SE), which correspond to successive ductile and brittle deformation phases. In the metasediments, three phases (D1–D3) were identified: D1 marked by schistosity and shear planes, D2 by crenulation schistosity linked to NNE-SSW compression, and D3 by late brittle faults including the Dimbokro shear zone. In the gneiss formations, four phases (Dn–Dn+3) were recorded, with Dn+1 characterized by foliation, shear planes, and folds, Dn+2 by open folds and dextral shear zones, and Dn+3 by brittle strike-slip faults and conjugate joints. These structures reveal a polyphased tectogenesis dominated by transpressive and compressive regimes. The Brobo shear zone and the Dimbokro fault emerge as major tectonic features controlling regional deformation. The results not only clarify the tectonic evolution of the Ivorian Birimian basement but also provide new insights into the geodynamic framework of the West African Craton, with implications for mineral exploration and regional tectonic correlations.

Citation: ***Salwa M Alfituri and Aisha M Alfituri.* 2026.** "Removal of Nutrient Salts: Comparative Study of Biosorbents Derived from Cocoa and Rubber Agricultural Wastes", *Asian Journal of Science and Technology*, 17, (06), 14360-14367.

INTRODUCTION

The Birimian basement of Côte d'Ivoire, which forms part of the West African Craton, is renowned for its tectono-metamorphic complexity and its major role in understanding Paleoproterozoic processes. These formations, dated around 2.1 Ga, consist of granitoids, migmatitic gneisses, and metasediments, and they bear witness to a polyphased evolution marked by compressive and transpressive regimes (Doumbia, 1997). The study of mesostructures within these units is essential, as they serve as privileged markers of deformation and allow for the reconstruction of regional geodynamic history. Moreover, tectonic structures play a decisive role in the localization of gold mineralization, which gives these investigations both economic and strategic importance (Allialy *et al*., 2023). Nevertheless, despite significant advances, several shortcomings remain in scientific literature. Research conducted in certain Birimian regions of Côte d'Ivoire, such as Boundiali (Djroh*et al*., 2022) or Bondoukou-Tanda (Koffi *et al*., 2024), has highlighted local tectonic phases but has not provided a systematic correlation between metasediments and granito-gneiss formations. Furthermore, studies on the Kan granito-gneissic complex (KGC) have mainly focused on petrogenesis and magmatic processes (Teha *et al*., 2024), leaving aside detailed structural analysis and its relationship with major regional shear zones. The Comoé metasediments (CMS), on the other hand, have been investigated from a geochemical perspective to trace their sources (Teha *et al*., 2023), but their tectonic evolution remains poorly documented, which limits the overall understanding of tectogenesis in this part of the Birimian basement.This gap is even more significant given that major structures such as the Brobo shear zone and the Dimbokro fault, identified by Bi Seydou *et al*. (2018), appear to play a key role in regional tectonic evolution. Yet, their relationship with the deformation phases recorded in both metasediments and gneisses has not been sufficiently explored. The absence of integrated studies combining teleanalytic data with field observations therefore represents a major limitation in the comprehension of deformation mechanisms.In this context, the present study proposes a thorough analysis of the mesostructures of the KGC and the CMS. The aim is to characterize ductile and brittle deformation markers, reconstruct the different tectogenetic phases, and highlight the major structures that controlled regional geodynamic evolution. By adopting an integrated approach that combines teleanalytic mapping with structural field measurements, this work seeks to fill the gaps left by previous studies and provide new insights for correlation with other segments of the West African Craton. Thus, it contributes to a better understanding of the polyphased tectogenesis of the Ivorian Birimian basement and opens perspectives for both mineral exploration and geodynamic research at the continental scale.

MATERIALS AND METHODS

Study site: The study area is located in central Côte d'Ivoire, within the Toumodi department, bounded by Abigui to the north, Moronouand Akakro to the south, Dimbokro to the east, and Toumodi to the west. It covers approximately 1000 km² (Fig. 1). The hydrographic network is dominated by the N'Zi River to the east and its tributary, the Kan River to the north. Geologically, the area belongs to the West African Craton (WAC), which evolved through two major stages: the formation of an Archean crust (3.5–2.5 Ga) and a Paleoproterozoic crust (2.2–1.7 Ga) resulting from the accretion of island arcs and oceanic plateaus during the closure of oceanic basins (Hirdes *et al*., 1992; Ledru *et al*., 1994). The WAC is bordered by Pan-African mobile belts (600 ± 50 Ma), including the Rockélides, Mauritanides, Trans-Saharan belt, and Anti-Atlas. Within Côte d'Ivoire, the craton is represented by the Man Shield, subdivided into two domains: the Archean Kenema-Man and the Paleoproterozoic Baoulé-Mossi, separated by the Sassandra fault. The Archean domain is composed of tonalitic gneisses, granulites, and charnockites, intruded by late granites, and structured by the Léonien (3.5–2.9 Ga) and Libérien (2.9–2.6 Ga) orogenies. The Paleoproterozoic domain consists of Birimian formations (2.5–1.8 Ga), including metavolcanic and metasedimentary belts associated with TTG batholiths and later granites. These formations were affected by the Eburnean orogeny (2.16–2.02 Ga), which produced polyphase deformation and metamorphism. Structurally, the Baoulé-Mossi domain records three major deformation phases: D1, related to early plutonic emplacement in an extensional to weakly compressive regime; D2, associated with NW–SE compression forming major folds and shear zones; and D3, marked by crenulation schistosity oriented N120°. Within this framework, the KGC occupies a central position in Côte d'Ivoire, between the Toumodi-Fètèkro volcano-sedimentary belt to the east and the Comoé basin to the west. It extends over ~100 km in length and ~20 km in width (Daouda, 1998). The complex is composed mainly of migmatitic and mylonitic gneisses, with basic intrusions and xenoliths (Fig. 1). Its origin has been debated: Mortimer (1990, 1992) considered it equivalent to Dabakala gneisses (Burkinian substratum), while Daouda (1998) argued it is a syntectonic granitoid emplaced within a transcurrent system. The Kan Complex thus represents a key witness to the Paleoproterozoic evolution of the Man-Léo Shield. Its structures and deformation patterns are consistent with the regional tectonic framework of the Baoulé-Mossi domain, shaped by the Eburnean orogeny and subsequent tectonic reactivations.In Côte d'Ivoire, the Baoulé-Mossi domain is expressed as volcano-sedimentary basins oriented N020°–N050°, composed of metavolcanic rocks (basalts, andesites, rhyolites), metasediments (turbidites, schists, quartzites), and granitoids.

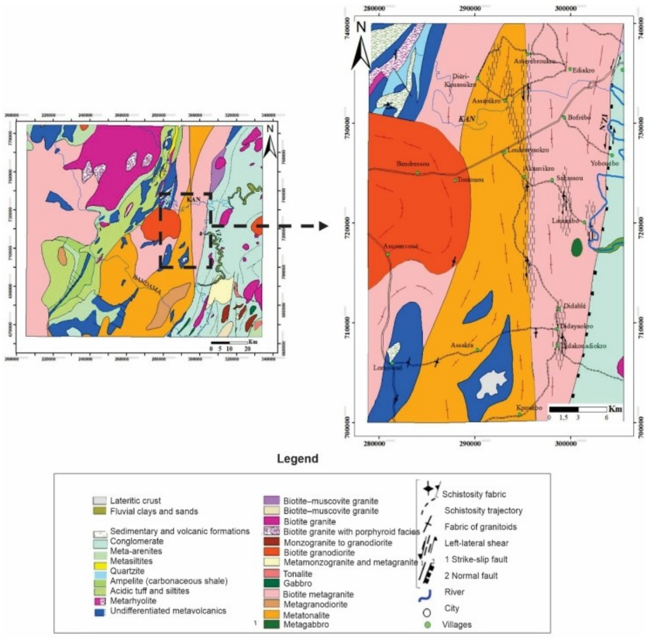

Figure 1. Cartes géologiques montrant le complexe granito-gneissique du Kan

Structural studies reveal three major deformation phases: D1, related to early plutonic emplacement in an extensional to weakly compressive regime; D2, associated with NW-SE compression forming major folds and shear zones; and D3, marked by crenulation schistosity oriented N120°. Thus, the Kan Complex is situated within the Paleoproterozoic Baoulé-Mossi domain of the Man Shield, recording the imprint of the Eburnean orogeny through granito-gneissic formations, migmatites, and mylonitic gneisses, all shaped by polyphase deformation and metamorphism.

METHODOLOGY

The lithological and structural study of the Assounvoué–Laourébo–Kpouébo–Assérébroukro area involved fieldwork and laboratory investigations, complemented by remote sensing and microstructural analyses.

Fieldwork: Sampling campaigns were conducted in August 2016, November 2016, and January 2018, using geological hammers, sledgehammers, and chisels. A total of 68 samples were collected from various outcrops, with GPS coordinates recorded and orientation noted for deformed rocks. Macroscopic descriptions allowed identification of lithological units.

Lineament Analysis: Lineament analysis was carried out using remote sensing techniques, based on a Landsat 8 image acquired (Fig. 2). The image was selected for its low cloud cover, ensuring better visibility of geological structures. Preprocessing included radiometric and atmospheric corrections (clouds and haze) performed with ENVI 5.3, converting pixel values into reflectance. Contrast enhancement was achieved through linear stretching, rescaling values from 0 to 255.A Principal Component Analysis (PCA) was applied to six multispectral bands (OLI2–OLI7, 30 m resolution), producing an enhanced image that highlights geological features such as fractures and drainage networks. Directional Sobel filters (7×7) were then applied in N–S, E–W, NE–SW, and NW–SE orientations to reinforce lineament visibility (Jourda, 2005; Jourda*et al*., 2006). Lineament extraction was performed by manual photo-interpretation, following the methods described by Raj (1989), Arlegui & Soriano (1998), and Suzan & Toprak (1998). The resulting lineament map (Fig. 3) was validated against field observations, existing geological and topographic maps, and infrastructure data (roads, power lines). Finally, a geostatistical study was conducted on the lineament map using Rockworks software, allowing the construction of rose diagrams(Fig. 3). These diagrams highlight the principal orientations and form the basis for regional structural interpretation.

Structural analysis methods:Remote sensing employed a Landsat 8 image (07 January 2019), radiometrically and atmospherically corrected using ENVI 5.3, then processed through Principal Component Analysis (PCA) and Sobel directional filters for manual extraction of lineaments. The lineament map was validated by field observations and statistically analyzed with RockWorks.Mesostructural analysis involved measurements of foliations, schistosities, lineations, folds, boudins, fractures, and shear planes, which were plotted on maps and processed with GEOrient and Stereonet.Microstructural analysis, conducted under an optical microscope, focused on mica fish, intracrystalline microfracturing, and crystallization–deformation relationships, following the criteria of Spry (1969), Nicolas (1988), Bard (1990), and Passchier&Trouw (1995, 2005).Finally, deformation quantification was performed using Fry's (1979) center-to-center method, complemented by Flinn's (1962) diagram, on eight samples of gneiss and metasediments. This approach enabled characterization of the deformation ellipsoid and assessment of stress intensity.

RESULTS

Lineament analysis:The tele-analytical study produced a comprehensive lineament map (Fig. 3) and a directional rose diagram (Fig. 3), both of which reveal four dominant structural orientations that define the tectonic framework of the study area. The E–W to ESE–WNW lineaments are mainly associated with dextral ductile and brittle strike-slip faults, as well as fracture systems oriented N090°–

N110°, reflecting significant lateral displacement. The N–S to NNE–SSW lineaments correspond to sinistral shear planes (Cn+1), dextral shear planes (Cn+2), and foliation surfaces (Sn+1), together with brittle sinistral strike-slip faults trending N–S and the major sinistral Dimbokro fault, underscoring the importance of transpressive regimes in regional deformation. The NE–SW lineaments are linked to dextral ductile shear zones striking N050° and brittle dextral faults trending N060°, suggesting oblique compression and strike-slip reactivation. Finally, the NW–SE to NNW–SSE lineaments indicate the presence of dextral ductile shear zones and sinistral brittle faults oriented N120°, reflecting complex kinematic interactions and conjugate fault systems. Collectively, these orientations represent the principal axes of regional deformation and demonstrate the polyphased tectogenesis of the Ivorian Birimian basement, where alternating compressive and transpressive regimes have repeatedly shaped both ductile and brittle structures. This integrated structural framework confirms that the Kan granito-gneissic complex and the Comoé metasediments record a long-lived, multi-stage tectonic evolution controlled by major shear zones such as Brobo and Dimbokro.

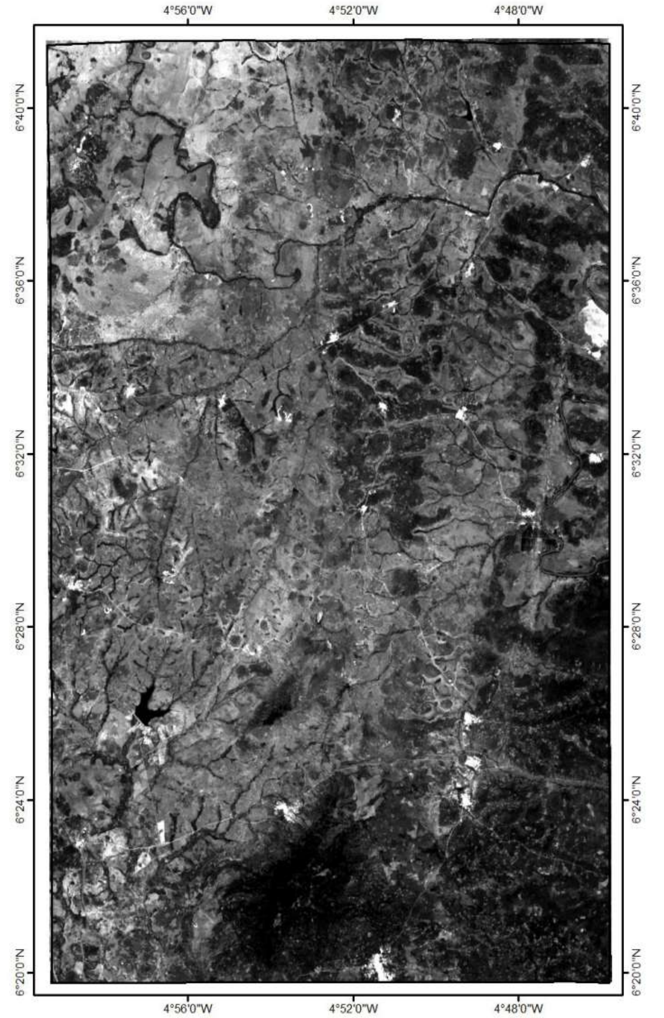

Figure 2. Landsat 8 image covering the study area, obtained after processing

Ductile deformation in Metasediments: The metasediments were affected by ductile deformation during the D1 and D2 deformation phases.

Markers of D1 deformation:

Flow schistosity (S1) and lineation L1:In the CMS, located along the eastern margin of the KGC, the primary stratification *(S0)* is defined at outcrop scale by centimeter- to decimeter-thick beds. It is oriented N–S to NNE–SSW (N05°–N15°) with a steep dip of about 70°E. This stratification was deformed during the first deformation phase *(D1)*, marked by the development of a flow schistosity (S1) parallel to S0 (Fig. 4). The *S1* schistosity is preferentially observed in mica-schists at Laourébo and Ahounianssou. It is characterized by the alignment of micaceous minerals, with orientation varying from one zone to another. At Laourébo, *S1* is oriented N–S to N10°, dipping steeply at 70°E (Fig. 5A and 5B).

The dip direction changes westward when moving away from the N'Zi River. At Ahounianssou, the flow schistosity is oriented N30° with a dip of 50°SE. The *S1* schistosity bears a mineral lineation *(L1)* that is submeridional and subhorizontal. In some cases, *L1* shows a gentle plunge of 5°–10°N in the mica-schists at Laourébo, and 10°–15°NE in those at Ahounianssou.

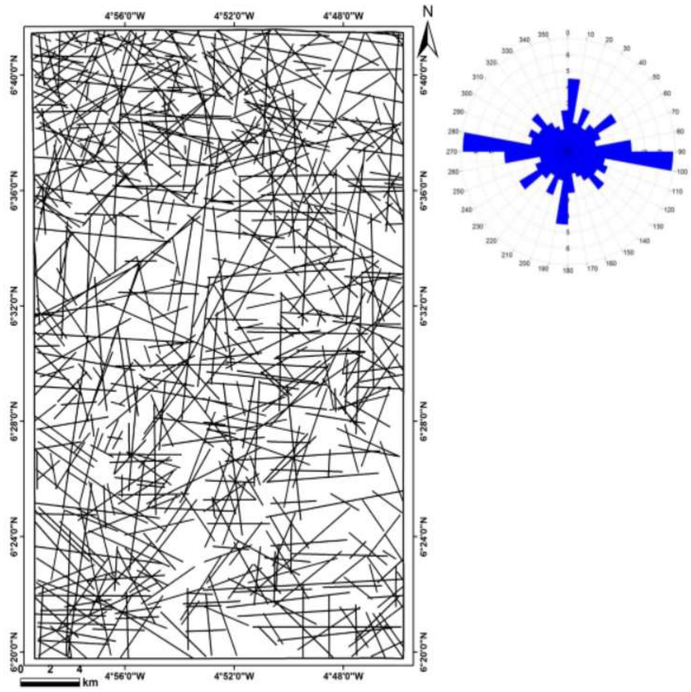

Figure 3. Lineament map of the study area and rose diagram showing the principal orientations of lineaments in the study area

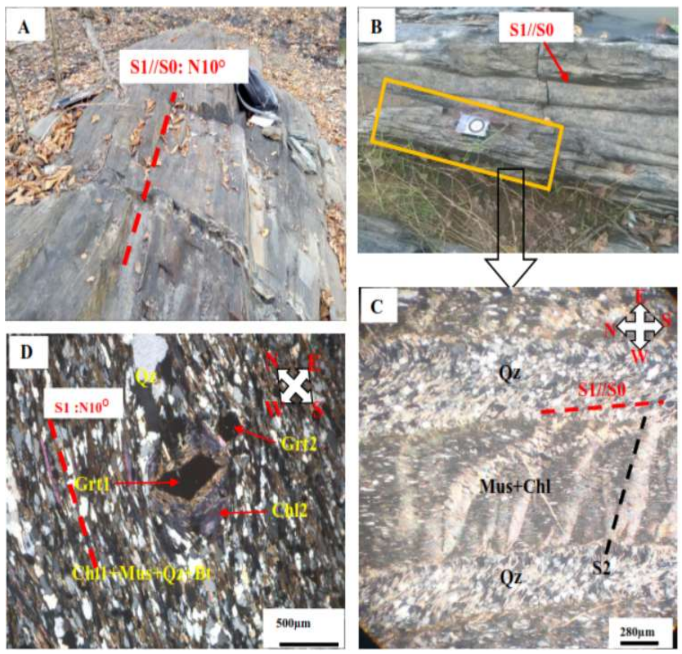

Figure 4. Macroscopic and microscopic aspects of structures observed in the metasediment. A: Centimeter- to decimeter-thick strata marking S0 in mica-schist; B: Macroscopic view showing S1 parallel to S0 in an arenite–pelitic facies; C: Alternation of quartzitic and pelitic beds. Note S1 parallel to S0 with superimposed S2 in an arenite–pelitic facies; D: Pre-tectonic garnet porphyroblast with a chlorite corona in mica-schist

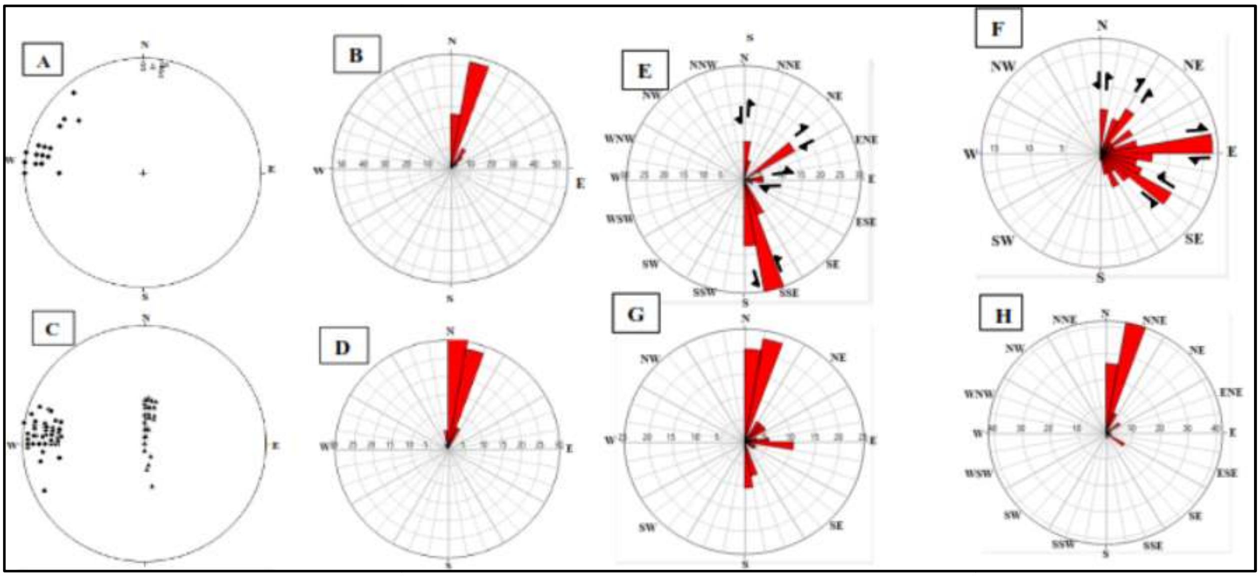

Figure 5. Stereograms and directional rose diagrams of structures. A: Poles of schistosity; S1 and lineation L1; B: Schistosity;C: Poles of foliation Sn+1 and lineation Ln+1;D: Foliation Sn+1; E: Ductile strike-slip faults; F: Strike-slip faults; G: Quartz veins;H: Pegmatite veins

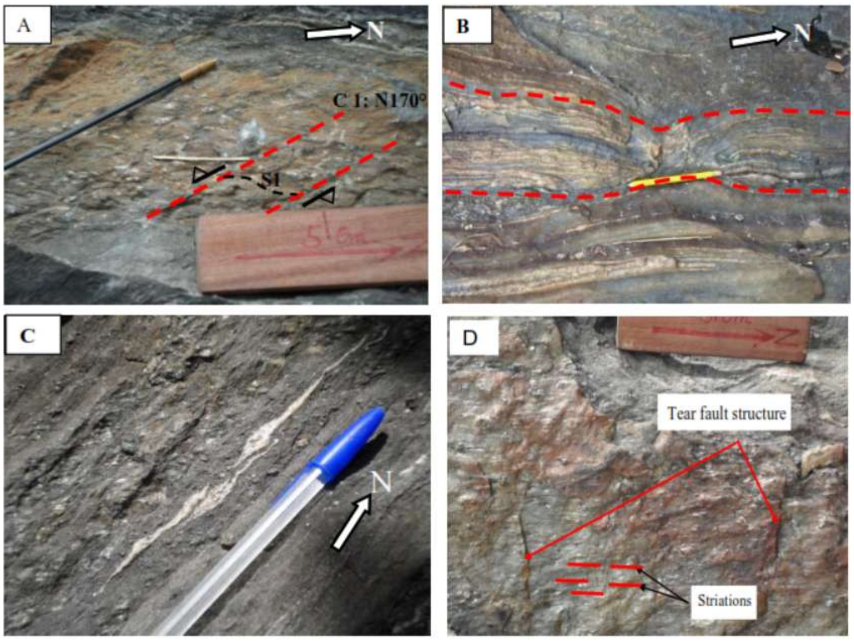

Figure 6. C/S structures and symmetrical boudins associated with D1 deformation. A: C1/S1 shear–schistosity planes in mica-schists; B: Symmetrical boudins in centimeter-thick layers; C: Symmetrical quartz vein boudins in mica-schists; D: Fault plane with striations and pull-apart features indicating a sinistral strike-slip fault

C1 Shear planes:The *D1* deformation in the metasediments is also expressed by the development of sinistral shear planes (*C1*) striking NNW–SSE (N170°). The juxtaposition of the *C1* shear planes with the *S1* schistosity results in the formation of *S/C* structures within the mica-schists (Fig. 6). These two planar fabrics are contemporaneous and were generated during the same transpressive *D1* deformation event.

Boudins associated with D1 deformation:The *D1* deformation is further evidenced by the occurrence of symmetric boudins affecting centimeter-thick layers interstratified with quartz veins. This type of boudinage is common in the mica-schists of Laourébo, where symmetric boudins of quartz veins are also observed (Fig. 6C). These boudins show no evidence of shear displacement along their interfaces. They are generally oriented N00°–N10°, parallel to the *S1* schistosity, and are indicative of constrictional deformation.

Markers of D2 deformation: The *S1* schistosity was subsequently reworked during a second deformation phase (*D2*), expressed by the development of a crenulation schistosity (*S2*) striking 110°. This fabric has been observed in the fine-grained facies of the arenite–pelitic formations in the Yobouébo area (Fig. 4C).

Brittle deformation markers in metasediments:Brittle deformation markers characterize a single late deformation phase (*D3*). This phase is expressed by E–W-oriented joints crosscutting the *S1* schistosity. It is also evidenced by a sinistral strike-slip fault trending NNE–SSW, identified in mica-schists at Laourébo.The fault plane strikes N10° with a steep, near-vertical dip and bears subhorizontal striations together with small-scale pull-apart structures (Fig. 6D). Similar subhorizontal striations are observed in the Kouadiotèkro area, within the contact zone between gneisses and metasediments. This regional NNE–SSW fault, located east of the Kan Complex, likely corresponds to the Dimbokro Fault. It also affects the gneisses along the eastern margin of the Kan Complex. The sense of movement is indicated by pull-apart features forming small staircase-like scales, consistent with sinistral strike-slip kinematics.

***Deformation markers in gneisses*:** The gneisses were affected by ductile deformation during successive phases (*Dn*, *Dn+1*, and *Dn+2*).

The structures associated with *Dn* deformation will be identified during the analysis of *Dn+1* markers.

Markers of Dn+1 deformation

Foliations Sn+1 and lineation Ln+1: At outcrop scale, the granito-gneissic formations of the Kan Complexexcluding the Toumodi granodiorite and felsic veins/dykesare affected by a foliation (*Sn+1*) related to the *Dn+1* deformation. This foliation displays characteristics similar to the *S1* schistosity observed in the metasediments along the eastern margin of the Kan Complex, i.e., submeridional orientation with a steep dip (Fig. 5C, 5D). Locally, the dip is gentler, ranging from 60° to 70°E.The*Sn+1* foliation is defined by alternating millimeter- to centimeter-thick layers of contrasting mineralogical composition (Fig. 7A). Light-colored layers consist of quartz and feldspar, whereas dark layers are enriched in biotite and commonly amphibole. This foliation is well developed in migmatitic gneisses from Akunvikro, Sahué, Loukouyaokro, and Assérébroukro. The *Sn+1* foliation bears a mineral lineation (*Ln+1*) that is subhorizontal, with a gentle plunge of 5°–10°N (Fig. 5C). This lineation, observed in Akunvikro, Sahué, and Assérébroukro, is associated with the stretching of quartz and biotite (Fig. 7C). The coexistence of foliation and mineral lineation imparts an *S–L* fabric to the gneisses of the Kan Complex, particularly the migmatites. This fabric is interpreted as the product of simple shear deformation.

Cn+1 shear planes:The *Sn+1* foliation is overprinted by a syn-*Dn+1* deformation expressed through the development of sinistral shear planes (*Cn+1*), clearly recorded in the gneissic formations. These planes strike submeridionally (NNW–SSE to NNE–SSW) with a steep dip, either vertical or gently inclined eastward (ca. 70°E), and are therefore parallel to *Sn+1*. The *Cn+1* shear planes strongly structure the gneissic formations, often obscuring traces of *Sn+1*. Pegmatite veins derived from thermotectonic differentiation are contemporaneous with this shear system, their differentiation planes corresponding to *Cn+1* (Fig. 7A, B). This shear is well developed in the migmatitic gneisses of Akunvikro and Assérébroukro,and probably represents a marker of the Brobo shear zone, previously defined further north by Lemoine (1988). The juxtaposition of *Cn+1* shear planes and *Sn+1* foliation produces well-defined *S/C* structures (Fig. 7A, B, 8A). Both surfaces carry distinct lineations: *Sn+1* bears stretching lineations marked by ribbon quartz and micaceous trails, while *Cn+1* carries slip striations typical of transcurrent shear. These two planar families are contemporaneous, formed during the same transpressive *Dn+1* event (Berthé*et al.*, 1979). The angle between *Cn+1* and *Sn+1* varies between 30° and 20°, depending on the intensity of mylonitization, decreasing to 10° or even becoming parallel in strongly mylonitized zones. In thin section, *Cn+1* planes are lined with muscovite and biotite, locally altered to epidote.

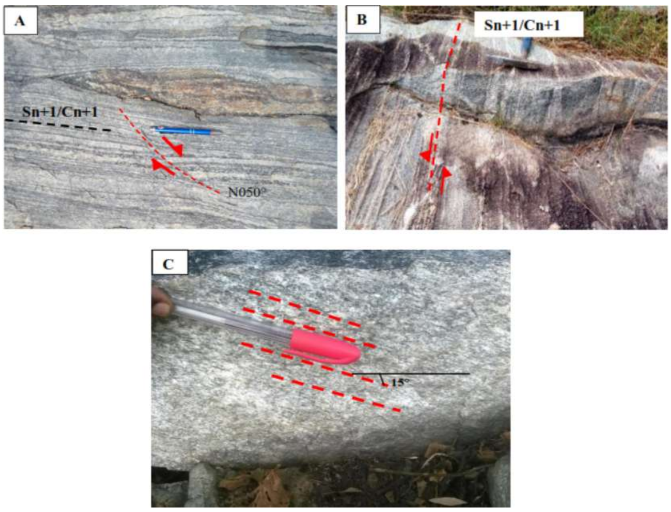

Figure 7: Photograph of the Sn+1 foliation and the Cn+1 shear plane in the migmatitic gneisses of Assérébroukro and Akunvikro. A: Sn+1 foliation parallel to the Cn+1 plane in the gneiss of Assérébroukro; B: Left-lateral Cn+1 shear plane parallel to the Sn+1 foliation plane in the gneiss of Akunvikro; C: Sn+1 foliation plane bearing a quartz–biotite lineation plunging 15° to the north

Pn+1 folds:The *Sn+1* foliation and sinistral *Cn+1* shear planes are parallel to the axial planes of similar folds (*Pn+1*). These folds deform an earlier foliation (*Sn*), transposed onto *Sn+1* (Fig. 8B), and are observed in migmatitic gneisses at Sahué. The *Pn+1* folds display vertical axes and axial planes oriented N10°–40°E (Fig. 8B, C), reflecting flattening deformation. The *Sn* foliation is absent in some gneissic formations (e.g., mylonitic gneisses of Laourébo, Yobouébo, Loukouyaokro), suggesting its development during an earlier *Dn* phase predating *Sn+1* and *Cn+1*. This *Dn* event is also absent in the CMS, implying that it preceded their deposition.Additional*Pn+1* folds are common in the migmatitic gneisses of the Kan Complex. Subhorizontal-axis folds frequently affect granitic leucosomes (Fig. 8D, E). The *Sn+1* foliation and *Cn+1* shear are subparallel to fold axial planes, producing axial-planar foliation. Axial planes are vertical, with fold axes plunging 5°–10°S. Intrafolial *Pn+1* folds of type “S” are frequent, with axial planes subparallel to foliation and vertical axes, serving as markers of sinistral *Cn+1* shear (Passchier&Trouw, 2005). Large symmetric *Pn+1* folds host parasitic folds: “S” and “Z” types on the limbs, and “M” type in the hinges (Fig. 8F). These parasitic folds are synchronous with *Dn+1* and are considered*Pn+1*. Shear along *Cn+1* planes affects fold limbs, producing sheared-limb and rootless folds, indicative of intense shear (Fig. 8C).

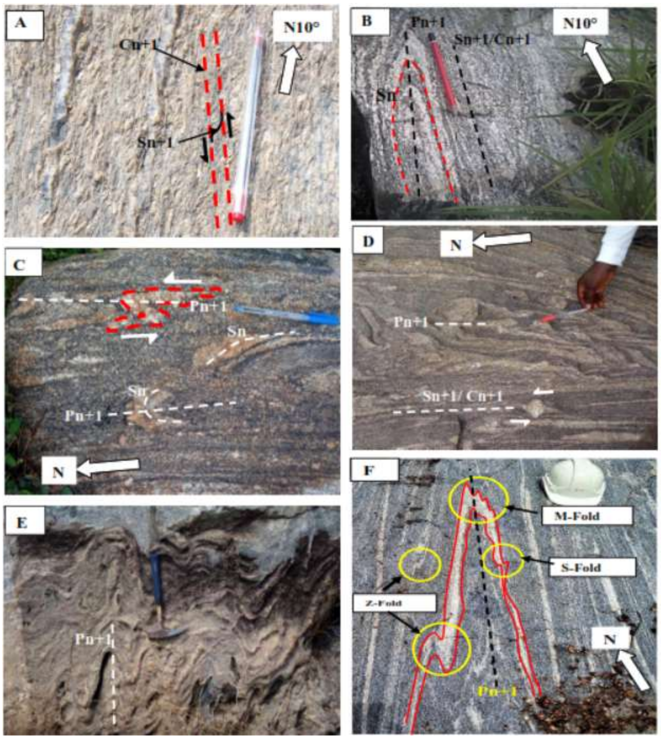

Figure 8. Photographs of Sn+1/Cn+1 planes and Pn+1 folds in gneisses. A: Sn+1/Cn+1 plane; B: Sn plane refolded by a Pn+1 folding event; C & D: Pn+1 folds with subhorizontal axes, observed respectively in horizontal and vertical sections; E: Intrafolial Pn+1 folds of “S” type and an isolated hinge fold; F: Symmetrical Pn+1 fold bearing parasitic folds—S- and Z-type on the limbs, and M-type at the hinge

Porphyroclasts and shear sense of Cn+1: At outcrop scale, porphyroclasts are mainly feldspathic and quartzose, occurring in migmatitic and mylonitic gneisses, as well as in pegmatite veins. They are predominantly of the delta (δ) type (Fig. 9A), according to the classification of Passchier&Trouw (2005). These monoclinic structures, together with intrafolial “S” folds, are key markers of sinistral *Cn+1* shear, formed by rotation of rigid feldspathic bodies. Antithetic microfractures are occasionally observed (Fig. 9C). Theta (ϕ) type porphyroclasts, with orthorhombic symmetry, also occur, marking flattening (Fig. 9B). Both structures result from the same transpressive *Dn+1* deformation. Rare sigma-type porphyroclasts, indicating dextral shear, are also present.

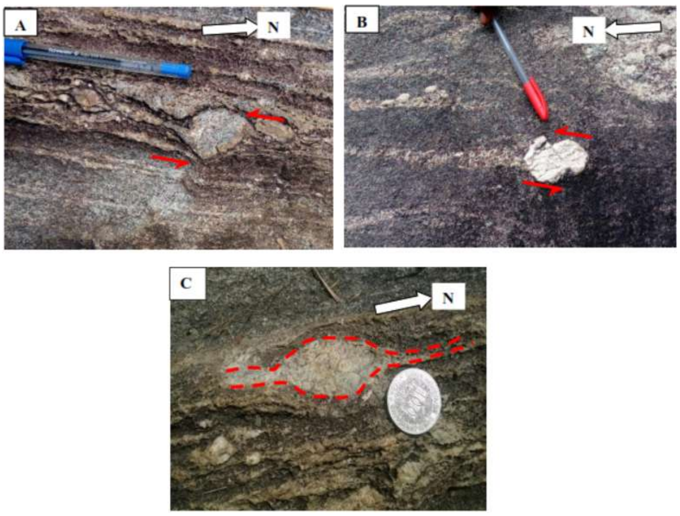

Figure 9. Photographs of porphyroclasts associated with Dn+1 deformation. A: Delta (δ) porphyroclast indicating a left-lateral sense of Cn+1 shear; B: Theta (ϕ) porphyroclast indicating flattening; C: Antithetic fracture within a delta (δ) porphyroclast, indicating a left-lateral sense of Cn+1 shear

Ductile strike-slip faults associated with Dn+1: The *Dn+1* deformation also produced several syn-*Dn+1* ductile strike-slip faults. Dextral faults are oriented N50° and N90°, while sinistral faults strike N10°, N110°, and N170° (Fig. 10A–F). Unlike *Cn+1*, these faults are irregular, non-penetrative, and centimeter- to decimeter-scale, observed in migmatites (Akunvikro, Assérébroukro) and metatonalite (Assakra, Lomo-sud). They developed progressively during *Dn+1*. The N170° orientation dominates in the study area (Fig. 5E), overprinting the shear direction defined by *S/C* structures. Dextral N50° faults are synchronous with NW–SE pegmatite dykes (Fig. 10F).

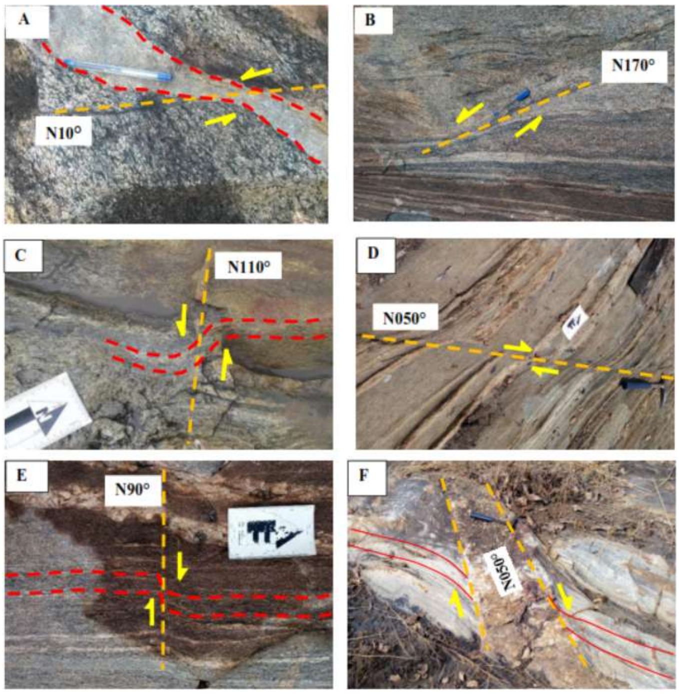

Figure 10. Photographs of ductile strike-slip faults associated with Dn+1 deformation in gneissic formations. A: Left-lateral ductile strike-slip fault trending NS to N10°; B: Left-lateral ductile strike-slip fault trending N170°; C: Left-lateral ductile strike-slip fault trending N110°; D: Right-lateral ductile strike-slip fault trending N50°; E: Right-lateral ductile strike-slip fault trending N90°; F: Pegmatite vein emplaced synchronously with the N05° ductile strike-slip fault

Boudins associated with Dn+1: The *Dn+1* deformation is also marked by symmetric and asymmetric boudins. Asymmetric shear boudins of quartz–feldspar material occurs in migmatitic gneisses at Akunvikro, antithetic to sinistral *Cn+1* shear (Fig. 11A). Symmetric quartz–feldspar boudins are also common (Fig. 11B), showing no slip along interfaces. Boudins are generally oriented N00° at Laourébo and N10° at Akunvikro, parallel to *Sn+1*, and indicative of constrictional deformation.

Markers of Dn+2 deformation: *Pn+2 folds:* The *Sn+1* foliation is folded during *Dn+2*, producing open *Pn+2* folds (Fig. 11C). Their axial planes strike N110°, parallel to *S2* crenulation schistosity in metasediments. These folds range from open-hinge to chevron-type, associated with NNE–SSW compression, and are observed in mylonitic gneisses at Loukouyaokro.

Cn+2 shear planes: The *Dn+2* deformation also produced dextral shear planes (*Cn+2*) striking NNW–SSE (N160°–N170°) (Fig. 11D), overprinting *Sn+1* and *Cn+1*. These planes are synchronous with *Pn+2* folding and were identified in mylonitic gneisses at Loukouyaokro. They also reflect NNE–SSW compression.

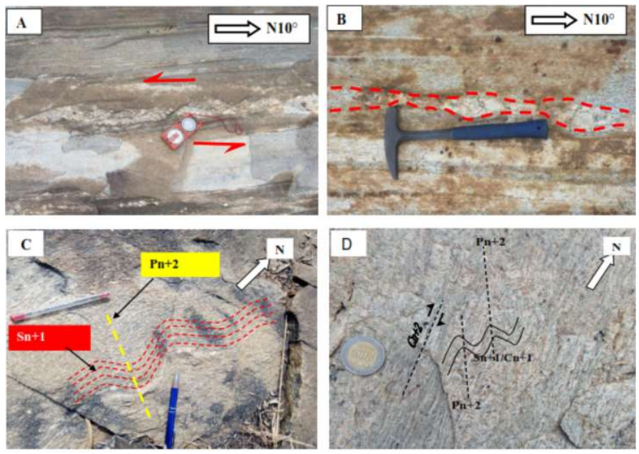

Figure 11. Aspects of different types of boudins associated with Dn+1 deformation in gneisses. A: Asymmetric boudins with antithetic fractures in the gneiss of Akunvikro; B: Symmetric pegmatite boudins in the gneiss of Akunvikro; C: Sn+1 foliation refolded by a Pn+2 folding event; D: Sn+1/Cn+1 planes refolded both by a Pn+2 fold and by a right-lateral Cn+2 shear plane

Brittle deformation markers in gneisses: Brittle deformation in gneisses is expressed at outcrop scale by tension gashes, strike-slip faults, and joints. Except for tension gashes associated with *Dn+1*, brittle strike-slip faults and joints represent markers of the late *Dn+3* deformation.

Tension gashes associated with Dn+1: Tension gashes related to *Dn+1* occur in mylonitic gneisses at Laourébo and Kouadiotèkro, near the contact with CMS. They are filled with recrystallized quartz. Two main families are distinguished (Fig. 12A): (i) large gashes with oblique fibrous structures, oriented N90°–N100° (Fig. 12B), and (ii) smaller gashes oriented N120°–N130°, tapering at the margins of first-order gashes. Both families are contemporaneous, formed under E–W to WNW–ESE compression.

Brittle strike-slip faults and joints associated with Dn+3: The *Dn+3* deformation represents a late tectonic phase that overprints all previous ductile structures. It is expressed by the development of brittle strike-slip faults, both dextral and sinistral, as well as conjugate joint systems. Brittle strike-slip faults affect all lithologies across the study area, from the granodiorite in the west to the metasediments of the Comoé Basin in the east, including gneisses and amphibole–pyroxenite intrusions. The deformation is particularly intense in the mylonitic gneisses of Laourébo, likely related to reactivation of the N'Zi Fault. Dextral strike-slip faults are oriented N90° and N060°, while sinistral faults strike N00°–N10° and N120° (Fig. 5F).These brittle faults occur in multiple generations. The earliest generation is represented by sinistral faults striking N120°. These were subsequently reworked by a second generation of dextral faults oriented N90° (Fig. 12C). A third generation of sinistral N–S faults followed, frequently associated with quartz veins. Finally, a fourth generation of dextral faults striking N60° (Fig. 12D) crosscuts the N–S faults. The N120° and N060° orientations often show dextral kinematics, suggesting reactivation of these fault sets. Such reactivations are particularly well developed in the Assounvoué granodiorite. Stereographic projections of fault orientations highlight dominant E–W (N90°) and NW–SE (N120°) trends (Fig. 5F). Along E–W dextral strike-slip faults, chlorite crystallization is commonly observed.The*Dn+3* deformation also produced two families of conjugate joints. The first set is oriented E–W, while the second strikes N–S. These joints are less abundant than the brittle faults but are frequently associated with quartz veins. Quartz veins parallel to joints are most commonly aligned N–S to NNE–SSW (Fig. 5G).

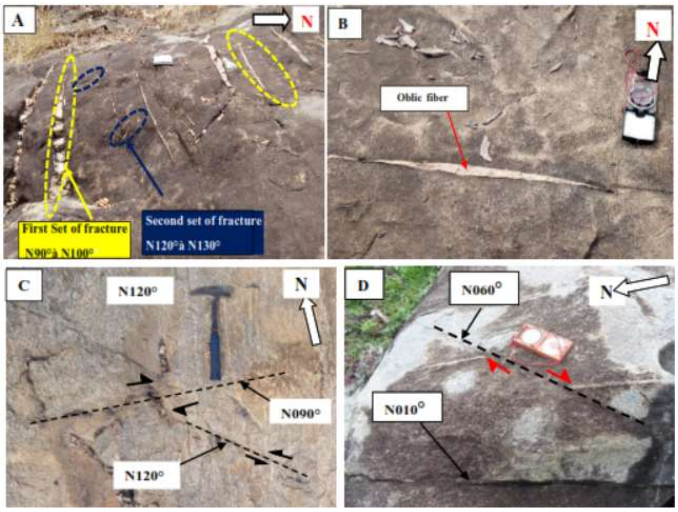

Figure 12. Photographs of tension fractures associated with Dn+1 deformation in the mylonitic gneiss of Laourébo. A: Family of fractures trending N090° and family of fractures trending N120°; B: EW-oriented tension fractures with oblique fibrous structure; C: Left-lateral strike-slip fault trending N120°, crosscut by a right-lateral strike-slip fault trending N090°; D: Right-lateral strike-slip fault trending N060°.

DISCUSSION

Structural organization of the KGC and the CMS: The lineament map and rose diagram reveal a complex structural framework, indicative of polyphased tectogenesis in the Kan granito-gneissic complex and the CMS. This evolution is strongly influenced by the Brobo and Dimbokro shear zones, which acted as major tectonic corridors guiding deformation and conditioning geological development. The principal lineament orientations (E–W, N–S, NE–SW, NW–SE) reflect successive stress regimes, ranging from WNW–ESE transpression to NNE–SSW compression. The NE–SW and NW–SE directions, linked respectively to dextral and sinistral strike-slip faults, suggest late reactivations and brittle adjustments.The metasediments record three deformation phases (D1–D3), illustrating a progressive evolution of stress. Phase D1, marked by schistosity S1 and sinistral shear planes C1, reflects WNW–ESE transpression, with symmetrical boudins confirming constrictional deformation. Phase D2, characterized by crenulation schistosity S2 oriented N110°, indicates NNE–SSW compression that reworks earlier fabrics. Phase D3, expressed by E–W joints and the sinistral Dimbokro fault, corresponds to a late brittle stage. Collectively, these phases highlight a transition from ductile transpressive deformation to brittle reorganization of regional stresses. The gneisses preserve a more complete tectonic record, with four phases (Dn–Dn+3). Phase Dn+1 is the most significant, marked by foliation Sn+1, sinistral shear planes Cn+1, intrafolial folds Pn+1, and δ- and ϕ-type porphyroclasts, all indicative of intense transpression associated with the Brobo shear zone. Quartz-feldspar boudins and ductile strike-slip faults confirm the coexistence of shear and constriction mechanisms. Phase Dn+2, with open folds Pn+2 and dextral shear planes Cn+2, reflects NNE–SSW compression and dextral reactivation of the Brobo corridor. Phase Dn+3, dominated by brittle strike-slip faults and conjugate joints, overprints earlier ductile structures and is likely associated with the opening of the Dimbokro fault. This succession demonstrates that the gneisses record a more comprehensive tectonic history than the metasediments, integrating both ductile and brittle deformation. These findings corroborate previous studies on the polyphased structuring of the Baoulé-Mossi domain and the West African Craton, where major shear zones are recognized as fundamental in tectonic evolution and in the emplacement of metamorphic and magmatic formations (Daï Bi *et al*., 2018; Ouattara *et al*., 2020; Teha *et al*., 2024). They also align with the broader Pan-African framework, characterized by transpressive deformation and late brittle reactivations that shaped regional shear zones (Benyahia *et al*., 2005; Nicollet, 2006). The correspondence between phases D1/Dn+1, D2/Dn+2, and D3/Dn+3 confirms a shared tectonic evolution in both metasediments and gneisses, reflecting continuous but variably expressed crustal dynamics in Côte d'Ivoire during the Paleoproterozoic. The Brobo and Dimbokro shear zones emerge as key structures controlling regional deformation, their successive sinistral and dextral reactivations illustrating the complexity and temporal reorganization of tectonic stresses.

Polyphased tectogenesis of the KGC and the CMS:The results highlight a polyphased tectogenesis dominated by transpressive and compressive regimes. This evolution is embedded within the Eburnean orogeny, which produced widespread polyphased deformation across the Baoulé-Mossi domain of the West African Craton (Ledru *et al*., 1994; Doumbia, 1997). The succession of ductile phases (D1–D2/Dn–Dn+2), followed by a late brittle stage (D3/Dn+3), illustrates a progressive transition from transpression to brittle reactivation, consistent with geodynamic models of island arc accretion and ocean basin closure (Hirdes *et al*., 1992). Similar dynamics have been documented in Boundiali and Bondoukou-Tanda, where late brittle reactivations contributed to crustal segmentation (Djroh*et al*., 2022; Koffi *et al*., 2024). In the gneisses, phase Dn+1, with its foliation, sinistral shear planes, and intrafolial folds, parallels structures in Dabakala and the Sassandra shear zone, reflecting syntectonic granitoid emplacement under transpression (Mortimer, 1992; Daouda, 1998).

Phase Dn+2, marked by open folds and dextral shear planes, corresponds to NNE–SSW compression and Brobo reactivation (Bi Seydou *et al*., 2018). Phase Dn+3, dominated by brittle strike-slip faults and conjugate joints, reflects late crustal segmentation and reactivation, comparable to Boundiali and Bondoukou-Tanda, where such structures are linked to gold mineralization (Djroh *et al*., 2022; Koffi *et al*., 2024). These correspondences confirm that the KGC and CMS are integral to the regional geodynamic model of the West African Craton, serving as key witnesses of Paleoproterozoic evolution and offering insights for both tectonic reconstruction and mineral exploration.

Geodynamic implications:The structural evolution of the KGC and CMS demonstrates an integrated tectonic history, where ductile and brittle phases are interconnected. This continuity bridges a gap in earlier studies that treated these formations separately (Teha *et al*., 2023; Teha *et al*., 2024). The coexistence of sinistral and dextral shear zones within the same domain reflects a transpressive regime, consistent with models of island arc accretion and ocean basin closure (Hirdes *et al*., 1992; Ledru *et al*., 1994). The dextral reactivation of the Brobo shear zone during Dn+2 underscores the role of major shear corridors in redistributing stresses and reorganizing regional tectonics (Bi Seydou *et al*., 2018). The late brittle phase Dn+3 highlights the importance of post-orogenic adjustments in the final structuring of the basement. Together, these findings emphasize the KGC and CMS as privileged records of Paleoproterozoic geodynamics, with implications for both continental-scale tectonic models and mineral exploration strategies.

CONCLUSION

The study of lineaments and tectonic structures in the KGC and the CMS reveals a polyphased tectogenesis organized around the Brobo and Dimbokro shear zones. The four principal lineament orientations (E–W, N–S, NE–SW, NW–SE) reflect successive stress regimes, from WNW–ESE transpression to NNE–SSW compression, followed by late brittle reactivations. The metasediments record three deformation phases (D1–D3), illustrating a transition from ductile to brittle deformation, while the gneisses preserve four phases (Dn–Dn+3), confirming a more complete tectonic history. The correspondence between D1/Dn+1, D2/Dn+2, and D3/Dn+3 highlights a shared tectonic evolution across both lithologies, reflecting continuous crustal dynamics in Côte d'Ivoire during the Paleoproterozoic. This polyphased structuring underscores the central role of regional shear zones in stress reorganization and in the emplacement of metamorphic and magmatic structures, situating the study area within a broader orogenic framework of the West African Craton.

REFERENCES

Allialy, K., Kouadio, B., & Yao, K. (2023). Gold mineralization and tectonic structures in the Birimian basement of Côte d'Ivoire. *Journal of African Earth Sciences, 198*, 104–118.

Arlegui, L. E., & Soriano, M. A. (1998). Characterizing lineaments from satellite images and field studies. *Tectonophysics, 312*(1–2), 37–55.

Bard, J. P. (1990). *Microtextures of igneous and metamorphic rocks*. Springer-Verlag.

Berthé, D., Choukroune, P., &Jegouzo, P. (1979). Orthogneiss, mylonite and non-coaxial deformation of granites: The example of the South Armorican shear zone. *Journal of Structural Geology, 1*(1), 31–42.

Bi Seydou, K., Kouadio, A., & Aka, F. (2018). Major shear zones and tectonic evolution in Côte d'Ivoire. *Bulletin de la Société Géologique de France, 189*(2), 123–136.

Daouda, K. (1998). *The Kan granito-gneissiccomplex:Petrographic and structural study*. Doctoral dissertation, University of Cocody, Abidjan.

Djroh, K., Kouadio, A., & Yao, K. (2022). Tectonic phases in the Boundiali region (Northern Côte d'Ivoire). *African Geoscience Review, 29*(3), 211–228.

Doumbia, S. (1997). *Tectono-metamorphic evolution of the Birimian basement of Côte d'Ivoire*. Doctoral dissertation, University of Montpellier II.

Fry, N. (1979). Random point distributions and strain measurement in rocks. *Tectonophysics, 60*(1–2), 89–105.

Hirdes, W., Davis, D. W., & Eisenlohr, B. N. (1992). The 2.1–2.2 Ga magmatic and tectonic events in the Birimian of West Africa. *Precambrian Research, 56*(1–2), 1–23.

Jourda, J. P. (2005). *Remote sensing methods applied to lineament studies*. University of Cocody.

Jourda, J. P., Kouadio, B., & Yao, K. (2006). Remote sensing and GIS in structural geology studies. *African Journal of Earth Sciences, 45*(2), 145–160.

Koffi, K., Kouadio, A., & Yao, K. (2024). Structural evolution of the Bondoukou-Tanda Birimian formations. *Journal of Geodynamics, 170*, 101–115.

Ledru, P., Milesi, J. P., Feybesse, J. L., Dommanget, A., & Marcoux, E. (1994). Geology of the Birimian belt of West Africa. *Geological Society Special Publication, 95*, 57–74.

Lemoine, S. (1988). *The Brobo shear zone: Structural study and tectonic implications*. DEA thesis, University of Paris VI.

Mortimer, N. (1990). Granitoid emplacement in the Dabakala region. *Precambrian Research, 47*(3–4), 257–274.

Mortimer, N. (1992). Syntectonic granitoids of the Burkinian substratum. *Journal of African Earth Sciences, 14*(2), 123–135.

Nicolas, A. (1988). *Principles of rock deformation*. Springer-Verlag.

Passchier, C. W., &Trouw, R. A. J. (1995). *Microtectonics*. Springer-Verlag.

Passchier, C. W., &Trouw, R. A. J. (2005). *Microtectonics* (2nd ed.). Springer-Verlag.

Raj, R. (1989). Lineament analysis in structural geology. *Tectonophysics, 162*(1–2), 1–12.

Spry, A. (1969). *Metamorphic textures*. Pergamon Press.

Suzan, S., & Toprak, V. (1998). Remote sensing in tectonic lineament studies. *International Journal of Remote Sensing, 19*(10), 1909–1920.

Teha, K., Kouadio, A., & Yao, K. (2023). Geochemical characterization of the Comoé metasediments. *Geochemistry: Exploration, Environment, Analysis, 23*(4), 567–582.

Teha, K., Kouadio, A., & Yao, K. (2024). Petrogenesis of the Kan granito-gneissic complex. *Precambrian Research, 389*, 107–123.

****